Supplemental Material for

Superior Mechanical and Thermal Properties of Oxygen Terminated Trigonal Mo_2B_2 MBenes

Di Zhao,[a] Mengqing Hu,[a] Ming Zhou,[a] Mingli Li,[a] Lei Zhang,[a] Oscar Allen,[a] Irfan Ali Soomro,[a] Samuel Akinlolu Ogunkunle,[a] Liang Wang,[a] Zhenzhen Wu,[a] Porun Liu,[a] Yuan Mei,[b] Yun Wang[a*]

[a] School of Environment and Science, Griffith University, Gold Coast Campus, Southport 4222, Australia

[b] CSIRO Mineral Resources, Kensington, WA 6151, Australia

* Corresponding author: Yun Wang, yun.wang@griffith.edu.au

A. Computation Process of Elastic Module

This paragraph demonstrates the basic modelling strategy for mechanical properties, including the calculation of elastic modulus. The modelling process is initiated within the MedeA VASP GUI interface by selecting the "MT - Elastic Properties" calculation type, as illustrated in Figure S4(a). Subsequent workflow construction occurs through the flowchart interface, beginning with the integration of Mechanical Properties module. Strain parameters are systematically assigned through this interface to establish deformation matrices (Figure S4(b)). Following strain configuration, force computation parameters are systematically defined using the MedeA VASP toolkit, ensuring proper convergence criteria and computational accuracy (Figure S4(c)). Final workflow implementation incorporates the VASP HT flowchart (Figure S4(d)).

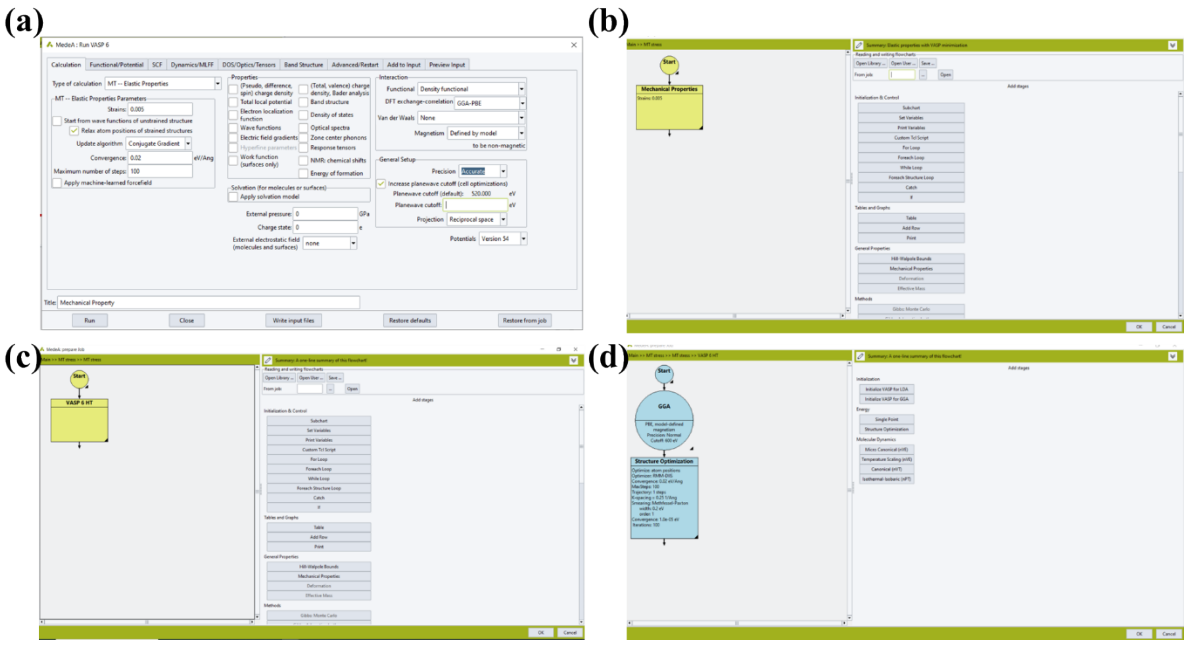

FIG. S1. The calculation of elastic modulus. (a) MedeA VASP GUI, (b) Mechanical properties module, (c) Flowchart interface, (d) VASP HT flowchart

B. Structural Properties of Mo_2B_2 and $Mo_2B_2T_2$ MBenes

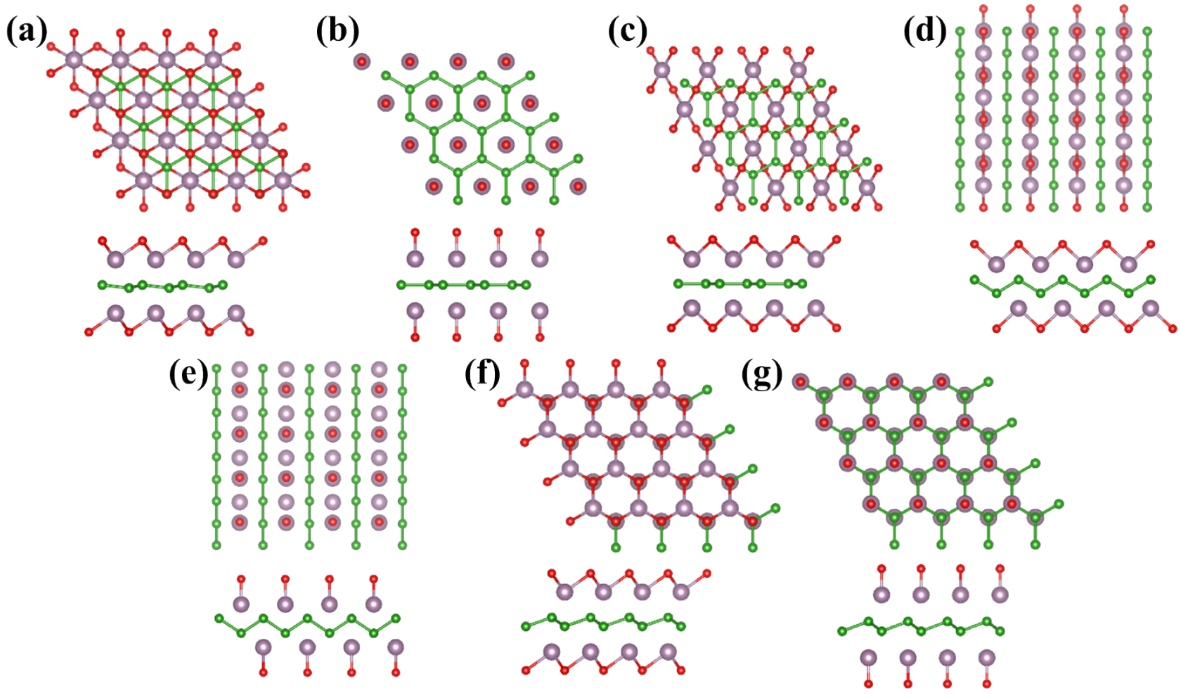

FIG. S2. Top and side views of different configuration models of -O terminated Mo_2B_2 MBene systems. (a) hexagonal $Mo_2B_2O_2$ model 1, (b) hexagonal $Mo_2B_2O_2$ model 2, (c) hexagonal $Mo_2B_2O_2$ model 3, (d) orthorhombic $Mo_2B_2O_2$ model 1, (e) orthorhombic $Mo_2B_2O_2$ model 2, (f) trigonal $Mo_2B_2O_2$ model 1, and (g) trigonal $Mo_2B_2O_2$ model 2. The Mo, B and O atoms are marked in purple, green and red, respectively.

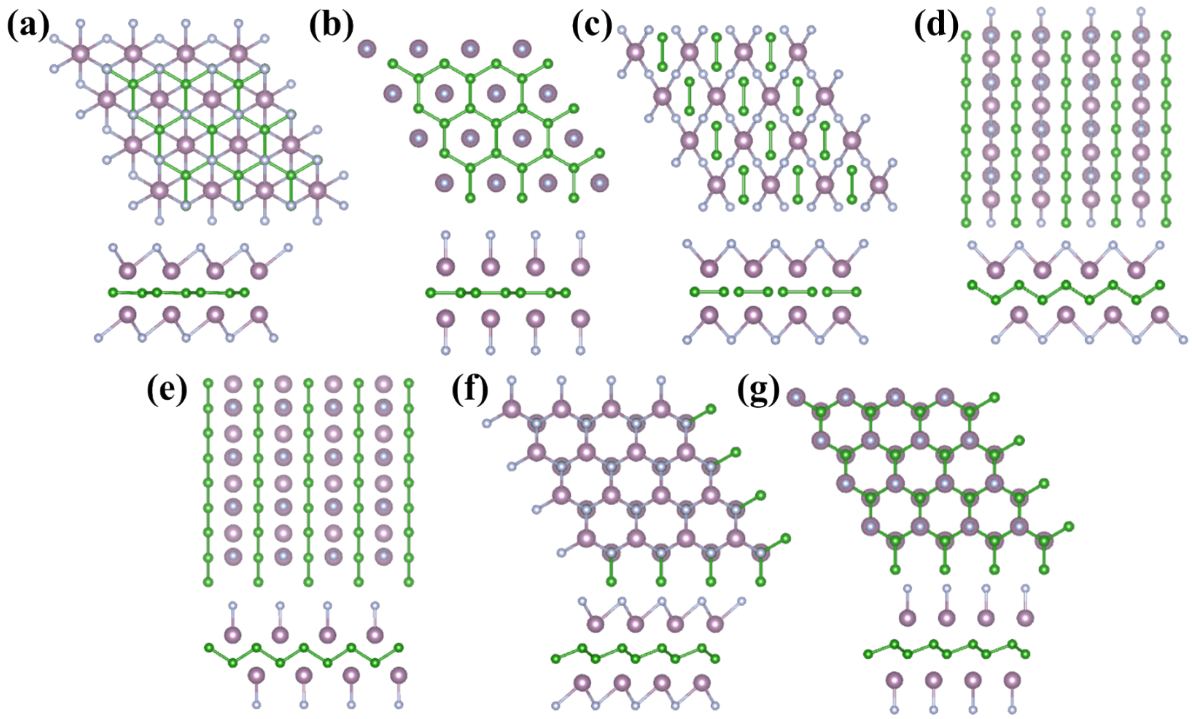

FIG. S3. Top and side views of different configuration models of -F terminated Mo_2B_2 MBene systems. (a) hexagonal $Mo_2B_2F_2$ model 1, (b) hexagonal $Mo_2B_2F_2$ model 2, (c) hexagonal $Mo_2B_2F_2$ model 3, (d) orthorhombic $Mo_2B_2F_2$ model 1, (e) orthorhombic $Mo_2B_2F_2$ model 2, (f) trigonal $Mo_2B_2F_2$ model 1, and (g) trigonal $Mo_2B_2F_2$ model 2. The Mo, B and F atoms are marked in purple, green and blue, respectively.

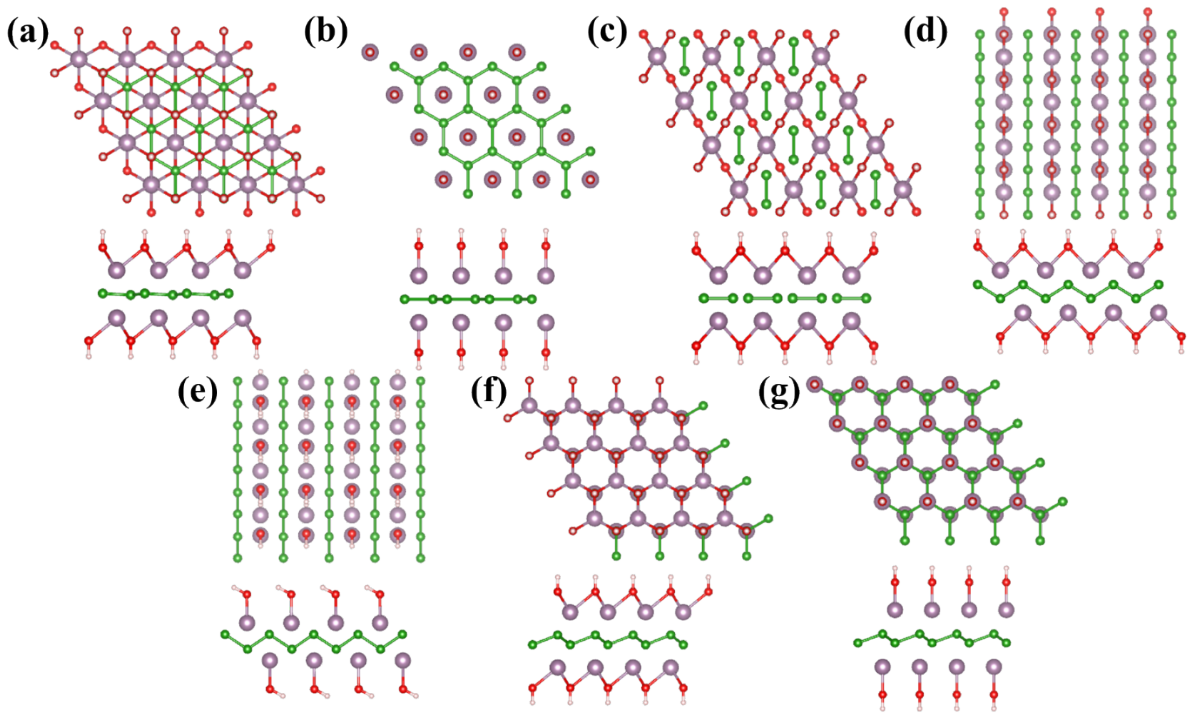

FIG. S4. Top and side views of different configuration models of -OH terminated Mo_2B_2 MBene systems. (a) hexagonal $Mo_2B_2(OH)_2$ model 1, (b) hexagonal $Mo_2B_2(OH)_2$ model 2, (c) hexagonal $Mo_2B_2(OH)_2$ model 3, (d) orthorhombic $Mo_2B_2(OH)_2$ model 1, (e) orthorhombic $Mo_2B_2(OH)_2$ model 2, (f) trigonal $Mo_2B_2(OH)_2$ model 1, and (g) trigonal $Mo_2B_2(OH)_2$ model 2. The Mo, B, O and H atoms are marked in purple, green, red and pink, respectively.

C. Calculated Elastic Constants

TABLE SI. Calculated elastic constants of Mo_2B_2

Phase	C_{11}	C_{12}	C_{22}	C_{66}
hex	245	41	245	102
orth	193	65	210	72
tri	244	110	244	64

TABLE SII. Calculated elastic constants of $Mo_2B_2T_2$-tri1

T	C_{11}	C_{12}	C_{22}	C_{66}
F	229	147	227	45
O	357	150	357	106
OH	318	74	319	125

D. Phonon Dispersion of $Ti_3C_2O_2$

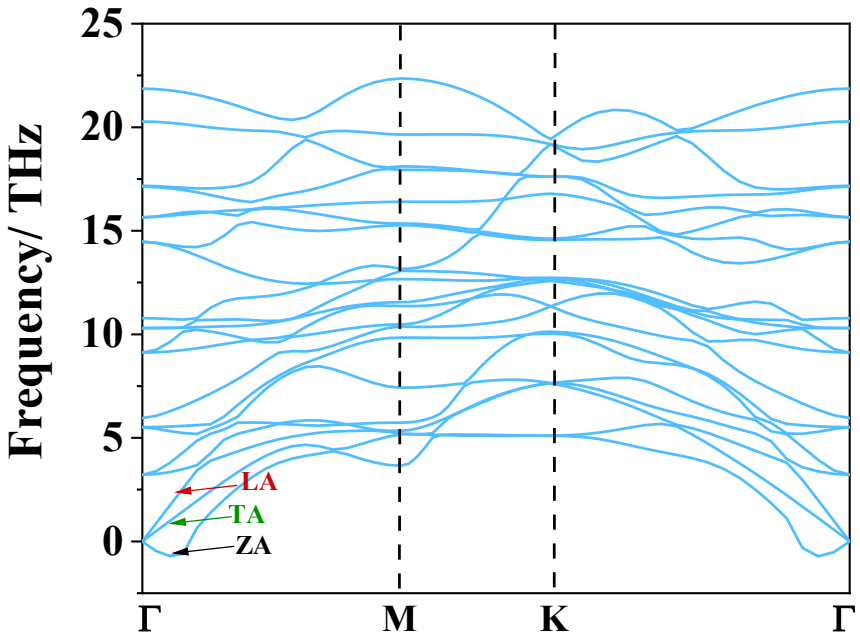

FIG. S5. Phonon dispersion of $Ti_3C_2O_2$